THE MODELLING OF A RESIDENTIAL BASED WIND POWERED GENERATOR

Adavbiele, A. S.
Department of Mechanical Engineering
Ambrose Alli University, Ekpoma, Edo State- Nigeria

Abstract
This study is concerned with the mathematical modelling of a residential based wind generator using a combination of actuator disc (AD), blade element momentum (BEM) and computational fluids dynamics (CFD). AD was used to evaluate the lift and drag coefficients as functions of local flow conditions. In order to determine the power output in relation to the turbine tip-speed ratio, radial variation of the flow condition and wake rotation, the BEM was used. However in pursuit of the most appropriate modelling strategy to handle the meshes of the 2D and 3D versions of the blade and the turbine assembly, CFD was applied and the results conceptualize the aerodynamics of the various wind turbine geometries at different speeds and how the specific blade and turbine assembly might behave in a real world application
.

Keywords: *Wind, energy, electricity, design, modelling.*

Background to the Study

The energy crisis of the 1970s and inter-generational ethical injunction in the Brundtland, which includes avoiding actions that might degrade the biosphere for future generations, have caused a revival of interest in wind energy (WCED, 1987; WEC, 1993; Johnson, 2006). Wind energy is a candidate in the quest for modular, abundant and affordable energy to provide power, especially in the rural areas far away from any existing electrical grid system in developing countries such as Nigeria. Using wind energy to power water pump, except in isolated areas is no longer invoked since the two variants of windmill technology (water pumping and electricity generation) can be met when enough electricity is generated, especially for a residential applications to provide light or little bit of power to earn extra income to work out of poverty. The technology development and the resulting price decline have caught the interest of a number of researchers that are now actively developing wind energy as one element of the balanced resource mix that serve both pumping and electricity needs (Johnson, 2006; Piggott, 2012; Gould, 2012). However, making a wind turbine may seem simple, but it is a big challenge to produce a wind turbine that meets specifications for standard electricity generation with each unit operating as an unattended power station and competes economically with other energy sources (Piggott, 2012). This means that a number of issues have to be addressed; however, for improved performance, this study aims to deal with the mathematical modelling of the complex fluid dynamics for a residential based horizontal axis wind turbine (HAWT).

Mathematical Modelling of the System

HAWT operates in a complex, inherently unsteady aerodynamic environment. The flow over the blades is dominated by three-dimensional (3D) effects, particularly during stall, which is accompanied by massive flow separation and vortex shedding (Kishinami, 2005; Mikkelsen, 2003; Ingram, 2011; Madsen, et al, 2007). There is always bluff-body shedding from the turbine nacelle and support structure which interacts with the rotor wake. In addition, the high aspect ratios of wind turbine blades make them very flexible, leading to substantial aero-elastic deformation of the blades, altering the aerodynamics. The aerodynamic theory is developed, starting with the simple one-dimensional momentum analysis of the actuator disc

(AD) and followed by the more detailed analysis of the blade element momentum (BEM) theory to design the blade geometry (Nayir, Rosolowski, & Jedut, 2010; Mughal, & Ullah, 2011). As AD and BEM methods are unable to accurately predict rotor loads near the edges of the operating envelope, a range of 2D/3D unstructured grid, with the help of a finite-volume Navier–Stokes, CFD techniques for predicting wind turbine performance characteristics have been developed (Nayir et al, 2010; Mughal & Ullah, 2011; Kaminsky et al, 2012; Mahawadiwar, et al, 2012; Leary, 2010; Versteeg & Malalasakera, 1995).

Having the cubic relation with the power, the wind speed is the most critical data needed to appraise the power potential of a candidate site. The wind is never steady at any site. It is influenced by the weather system, the local land terrain, time and season, and the height above the ground surface. Since the wind speed varies by the minute, hour, day, season, and year, and long term measurements are expensive, the short term, say one year, data is compared with a nearby site having a long term data to predict the long term annual wind speed at the site under consideration. The number of blades is often viewed as the blade solidity. Higher solidity ratio gives higher starting torque and operates at low speed. In order to operate more efficiently at high speed, large-scale wind turbines have low solidity ratio, with just two or three blades. The change in wind velocity with elevation above ground is the wind shear, . The turbine solidity, σ is defined as the ratio between the area of the blade to the area of the disk:

$$\sigma = bc(r)/2\pi r \qquad (1)$$

where b is the number of blades, c the chord length of the local blade section and r, the radius of the blade.
There are several technical parameters that are used to characterise windmill rotors, which must be understood to carry out appropriate design (Kaminsky et al, 2012). The value of Torque, T measured is the value of angular force acting on the miniature rotor blade. The tip speed ratio is a very important parameter for wind turbine design. It expresses the speed ratio, λ between the tip speed, Ω and the undisturbed wind speed, U.

$$\lambda = \Omega r/U\infty \qquad (2)$$

Drag devices always have tip-speed ratios less than one and hence turn slowly, whereas lift devices can have high tip-speed ratios and hence turn quickly relative to the wind. The wind power density, Pd is simply expressed as the amount of power available from the wind at a given speed and with area, A denoting the swept area of the rotor. A thrust coefficient, Tc could be defined for the integral thrust force, T acting on the rotor with air density, :

$$Tc = T/\tfrac{1}{2}\rho U2\infty A \qquad (3)$$

The kinetic energy in air of mass, m moving with speed, v is given by the power in moving air and is the flow rate of kinetic energy per second. Therefore, the power, P in the wind is given as (Kaminsky et al, 2012)

$$P = \frac{1}{2}m\dot{v}^2 = \frac{1}{2}\rho Av.v^2 = \frac{1}{2}\rho Av^3 = \frac{1}{8}\rho\pi d^2v^3 = \frac{1}{2}\rho Av_{rms}{}^3 \quad (4a)$$

$$P_{extracted} = \frac{1}{2}\dot{m}\left(v^2 - v_0^2\right) \quad (4b)$$

$$P_{rotor} = \frac{1}{2}\rho A\frac{v+v_0}{2}.\left(v^2 - v_0^2\right) = \frac{1}{2}\rho Av^3.\frac{\left(1+\frac{v_0}{v}\right)\left[1-\left(\frac{v_0}{v}\right)^2\right]}{2}$$

$$= \frac{1}{2}\rho Av^3.C_p \quad (5$$

where $P_{extracted}$ is the power extracted, C_p is p ower co -efficient or capacity factor and $\rho = P_r/RT = \rho_o\text{-}1.194x10^{-4}.H_m$ is the density in kgm $^{-3}$ and $T = 15.5 - \frac{19.83.H_m}{3048}$ in ◦C and H_m is the height of the wind turbine above sea level.

One of the variations of the approach is the actuator line model. The blade r elative velocity v_{rel} and incidence angle α are calculated from the local wind velocity components:

$$v_{rel} = \sqrt{v_z^2 + \left(\Omega r - v_\theta\right)^2} \quad (6)$$

while the lift, L and drag, D forces are respectively by:

$$L = \frac{\rho C_L v_{rel}^2}{2};\ D = \frac{\rho C_D v_{rel}^2}{2} \quad (7)$$

Axial, $\square_n$ and tangential, $\square_n$ forces acting on a blade segment are defined respectively as:

$\square_n = \square_n \square\square\square + \square_n \square\square\square$ (8a)

$\square_n = \square\square\square\square\square - \square_n \square\square\square$ (8b)

Subsequently, the height, h effect on the wind speed and power is given as:

$$v_2 = v_1\left(\frac{h_2}{h_1}\right)^\alpha \quad (9)$$

$$P_2 = P_1\left(\frac{h_2}{h_1}\right)^{3\alpha} \quad (10)$$

where α is ground surface friction co-efficient

The variation in wind speed is best described by the Weibull probability distribution function 'h' with two parameters: the shape parameter 'k', and the scale parameter 'c'. The probability of wind speed being v during any time interval is given by the following (Kaminsky et al, 2012):

$$h(v) = \left(\frac{k}{c}\right)\left(\frac{v}{c}\right)^{(k-1)} e^{-\left(\frac{v}{c}\right)k} = \frac{2v}{c^2}e.^{-\left(\frac{v}{c}\right)^2} = \frac{2v}{v_{mean}^2}e.^{-\left(\frac{v}{v_{mean}}\right)^2} \quad (11a)$$

$$v_{mean} = c\sqrt{1+\frac{1}{k}} \quad (11b)$$

$$v_{rms} = \sqrt[3]{\frac{1}{8760}\int_0^\infty hv^3 dv} \quad (11c)$$

$$P_{rms} = \frac{1}{2n}\sum_{i=1}^{n}\rho_i v_i^3 \quad (12)$$

where n is the number of observation in the averaging period and the subscript rms is root mean square.

The Actuator Disc Model

The ideal, frictionless efficiency of a wind turbine was predicted by A. Betz in 1920 using a simple one-dimensional (1D) model, known as the actuator disc approach, which uses the following assumptions:

(I) The flow is ideal and rectilinear across the turbine i.e. steady, homogenous, inviscid, irrotational, and incompressible.

(ii) Both the flow and thrust are uniform across the disk.

(iii) The static pressure at the upwind and downwind boundaries is equal to the ambient static pressure.

The actuator disc model is probably the oldest analytical tool for evaluating rotor performance. In this model, the rotor is represented by a permeable disc that allows the flow to pass through the rotor, at the same time as it is subject to the influence of the surface forces. The classical actuator disc model is based on conservation of mass, momentum and energy, and constitutes the main ingredient in the 1D momentum theory. By decomposing into its axial or streamwise, Ua and tangential, Ut components and introducing the induction factors a and a', the velocity vector is given by the relationships:

$$Ua = (1 - a)U\infty \quad (13a)$$

$$Ut = (1 + a')\omega r \quad (13b)$$

where $U\infty$ is the air free stream and ω is the angular velocity.

The design of modern wind turbines rely on the same aerodynamic principles as an aircraft - predicting lift and drag force in a challenging environmental conditions. Figure 1 depicts this idea. The turbine rotates with angular tip velocity Ω and tangential velocity Ωr. Wind with local velocity components vz and vɵ creates lift force L and drag force D, which at a correct incidence angle, turns around the turbine rotor. The rotor is represented by an actuator disc that creates a pressure discontinuity of local area Ao and local velocity vo (Mikkelsen, 2003). The control volume of the model is defined by a stream tube whose fluid passes through the rotor disc. The wind at the inlet to the model has an approach velocity v over an area A, and a slower downstream velocity v3 over a larger area A3 at the outlet. A simple schematic of the model is given in Figure 2.

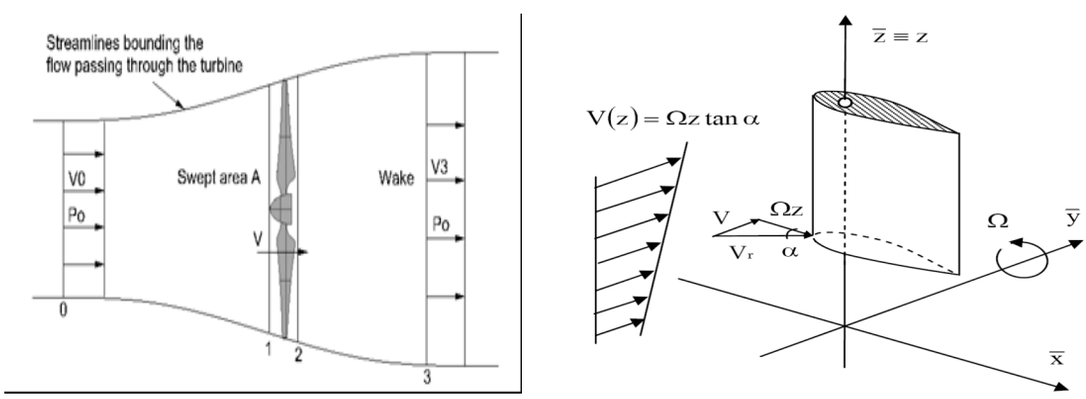

Figure 1: Control volume for the idealised actuator-disk Analysis

There are two primary physical principles by which energy can be extracted from the wind; these are through the creation of either drag or lift force (or through a combination of the two). Drag forces provide the most obvious means of propulsion, these being the forces felt by a person (or object) exposed to the wind. Lift forces are the most efficient means of propulsion but being more subtle than drag forces are not so well understood. The basic features that characterise lift and drag are: drag is in the direction of airflow and lift is perpendicular to the direction of airflow. The generation of lift always causes a certain amount of drag to be developed. With a good aerofoil, the lift produced can be more than thirty times greater than the drag. The lift devices are generally more efficient than drag devices.

The proportion of the power in the wind that the rotor can extract is termed the coefficient of performance (or power coefficient or efficiency; symbol Cp) and its variation as a function of tip speed ratio is commonly used to characterise different types of rotor. It is physically impossible to extract all the energy from the wind, without bringing the air behind the rotor to a standstill. Capacity factor is the ratio of the actual energy produced in a given period, to the hypothetical maximum possible, i.e. running full time at rated power. It is dependent upon wind speed versus the optimum performance characteristics of the turbine. Capacity factor is an indicator of how much energy a particular wind turbine makes in a particular place. Capacity Factor is not an indicator of efficiency. Consequently there is a maximum value of Cp of 59.3% (known as the Betz limit), although in practice real wind rotors have maximum Cp values in the range of 25%-45%.

Using Betz limit for an ideal frictionless turbine,

$$F = \rho Av(v - v_0) = A(pr_1 - pr_2);\ pr_1 - pr_2 = \frac{1}{2}\rho(v^2 - v_0^2) \quad (13)$$

$$P = Fv = 2m\,\&(v - v_0)v = 2Av^2(v^2 - v_0^2) \quad (14)$$

where ρ=1/v, $V = \frac{1}{2}(v + v_0)$ and F is the impact force.

A main motivation for developing such types of model is to be able to analyse and verify the validity of the basic assumptions that are employed in the simpler and more practical engineering AD model. The wind exerts an axial thrust, T on the turbine in the flow direction. An equal and opposite force is exerted by the turbine on the wind through its mounting with the ground. By applying a horizontal momentum relation between sections 0 and 3, see Figure 1, the thrust at the rotor disc, with diameter, Dr can be found. The fractional decrease in wind velocity between the free stream and rotor plane can be expressed in terms of an axial induction factor a:

$$a = (v - v_0)/v$$

$$P_{output} = 2Av^3a(1-a)^2 \quad (15a)$$

$$P = T\Omega \quad (15b)$$

Output power

$$P = T\omega = Tv/r = 2Tv/D_r \quad (15c)$$

where T is the turbine torque

The power coefficient (i.e. the extracted power over the total available power) is simply

$$C_p = \frac{P}{\frac{1}{2}\,\&mv^2} = 4a(1-a)^2$$

$$\frac{dC_p}{a} = 4(1-a)(1-3a) = 0 \quad (16)$$

giving maximum value of a=1/3 and 1.

Blade-Element Momentum

Wind turbine blades rely on lift produced by their airfoil cross sectional shapes to produce the torque at the base needed to turn the generator. The blade profiles, loads and performance calculations are today routinely performed by the Blade-Element Momentum (BED) method. This theory produces the angle of twist and chord length for a given airfoil cross section and rotation speed at a finite number of positions along the span of the blade. From these two dimensional sections a three dimensional shape can be extruded. The BEM theory accomplishes this by treating a given cross section as an independent airfoil, which processes wind with a speed and direction that is a vector sum of the oncoming wind speed and the

wind speed generated by rotation. The method is indeed computationally cheap and thus very fast, even with providing very satisfactory results. The BEM method consists on dividing the flow in annular control volumes and applying momentum balance and energy conservation in each control volume. The annuli are bounded by stream surfaces that enclose the rotor and extend from far upstream to far downstream.

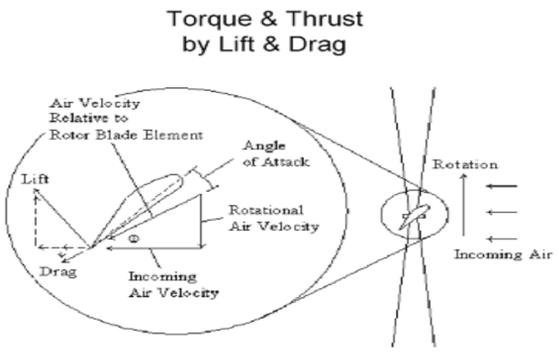

Figure 2: Blade Element Momentum Analysis

The impact of the rotating wake can be estimated by extending the Betz analysis to a 2D model in the radial direction. The control volume is divided into many non-interacting elementary radial blade sections that could be analysed independently by blade element method (BEM), (Ingram, 2011; Madsen et al, 2007). However, the following assumptions apply:

(i) The flow far upstream is purely axial; however there is a discontinuous jump in angular velocity across the rotor plane because torque is exerted on the rotor

(ii) The turbine wake rotates in the opposite direction to the rotor with an angular velocity, ω2

(iii) Basic assumptions of the method are that the induced velocity in the rotor plane is equal to one half of the induced velocity in the ultimate wake, and that the flow can be analysed by dividing the blade into a number of independent elements

(iv) Circumferentially averaged torque on a radial element is then,

$$dT = \omega r^2 dm \;\&= \omega r^2 (\rho v 2\pi)\, r dr \qquad (17a)$$

$$a' = \frac{\omega}{2\Omega} \text{ and } \lambda_r = \frac{\Omega r}{v} \text{ as given in equation (1)}$$

The torque produce by each blade is then obtained by integration in the radial direction:

$$T = F_\theta dr \qquad (17b)$$

$$= 4\pi\rho v \int_0^r (1-a) a' r^3 dr \qquad (17c)$$

$$a' = \frac{1}{2}\left(\sqrt{1 + \frac{4a}{\lambda_r^2})1-a) - 1} \right)$$

At the tip of the turbine blade losses are introduced in a similar manner to those found in wind tip vorticies on turbine blades. These can be accounted for in BEM theory by means of a correction factor. Four equations are used: two derived from momentum theory which expresses the axial thrust and the torque in terms of flow parameters:

$$dF_x = Q\rho v_1^2 [4a(1-a)]\pi r dr \qquad (18)$$

$$dT = Q\rho v\Omega [4a'(1-a)]\pi^3 r dr \qquad (19)$$

and the other two derived from a consideration of blade forces which express the axial force and torque in terms of the lift and drag coefficients of the aerofoil:

$$dF_x = \sigma' \pi \rho \frac{v^2 (1-a)^2}{\cos^2 \beta} (C_L \sin \beta + C_D \cos \beta) r dr \quad (20)$$

$$dT = \sigma' \pi \rho \frac{v^2 (1-a)^2}{\cos^2 \beta} (C_L \cos \beta - C_D \sin \beta) r^2 dr \quad (21)$$

where,

$$\frac{a}{1-a} = \frac{\sigma' (C_L \sin \beta + C_D \cos \beta)}{4Q \cos^2 \beta}$$

$$\frac{a'}{1-a} = \frac{\sigma' (C_L \cos \beta - C_D \sin \beta)}{4Q\lambda \cos^2 \beta}$$

Since most wind tunnels testing is done with the aerofoil stationary we need to relate the flow over the moving aerofoil to that of the stationary test. To do this we use the relative velocity over the aerofoil. In practice the flow is turned slightly as it passes over the aerofoil so in order to obtain a more accurate estimate of aerofoil performance an average of inlet and exit flow conditions is used to estimate performance (Pierce, 2008).

When using BEM as a design method, the following inputs and outputs are defined: input—rated power P, power coefficient CP , mean wind speed V0, number of blades B; output—rotor diameter D, chord ci(r) and twist θi(r) radial distribution. This is in principle the BEM method, but in order to get good results it is necessary to apply, at least, the two corrections below: The first is called Prandtl's tip loss factor, which corrects the assumption of an infinite number of blades. The second correction is called Glauert's correction and is an empirical relation between the thrust coefficient CT and the axial interference factor a for values of a greater than approximately 0.3, where the relation derived from the one-dimensional momentum theory is no longer valid.

Computational Fluid Dynamics

Consider a blade section in Figure 1 (ii) performing a steadily rotating motion. Two different reference systems are now introduced. One is a global reference system attached with the blade and moving with it. The second one is a local reference system, still fixed with the blade, but aligned point by point with the local tangential and normal directions of the blade surface.

In the first reference system the steady incompressible time–averaged Navier–Stokes equations for a rotating frame of reference are defined and numerically solved (Mahawadiwar et al, 2012; Leary, 2010):

$$\nabla . \bar{v}_r = 0 \quad (22)$$

$$\nabla . (\vec{v}_r \vec{v}_r) + 2\bar{\Omega} x \vec{v}_r + \vec{\Omega} x \bar{\Omega} x \vec{\tau} = -\frac{1}{\rho} \nabla p + \nabla . \tau + \bar{f} \quad (23)$$

where the relative velocity vector is $\bar{v}_r$, the rotational tip speed $\vec{\Omega} = 0$, the fluid density is ρ, the stress tensor is τ and the external body force is $\bar{f}$. The Coriolis force and the centrifugal force terms are identified respectively as $2\bar{\Omega} x \vec{v}_r$ and $\vec{\Omega} x \bar{\Omega} x \vec{\tau}$.

The second reference system refers to the boundary layer equations, which will be recalled in the post–processing step. In order to analyze the output data from the Navier-Stoke's (N–S) code, Fluent is used to evaluate the relative importance of the various terms in the boundary layer equations with respect to the arising of rotational effects. The wind turbine 3D incompressible boundary layer equations for a steady rotating blade flow, based on the Prandtl's boundary layer equations are:

$$\frac{\partial u}{\partial x}+\frac{\partial u}{\partial y}+\frac{\partial w}{\partial z}=0 \qquad (24)$$

$$u\frac{\partial \overline{u}}{\partial x}+v\frac{\partial \overline{u}}{\partial y}+w\frac{\partial \overline{u}}{\partial z}=\frac{1}{\rho}\frac{\partial \overline{p}}{\partial x}+2\Omega\omega\cos\theta+\Omega^2\bar{x}\cos\theta+\frac{\partial}{\partial y}\left(v\frac{\partial u}{\partial y}-\overline{u'v'}\right) \qquad (25a)$$

$$u\frac{\partial \overline{u}}{\partial x}+v\frac{\partial \overline{u}}{\partial y}+w\frac{\partial \overline{u}}{\partial z}=\frac{1}{\rho}\frac{\partial \overline{p}}{\partial y}+2\Omega\omega\cos\theta+\Omega^2\bar{y}\cos\theta+\frac{\partial}{\partial z}\left(w\frac{\partial v}{\partial z}-\overline{v'w'}\right) \qquad (25b)$$

$$u\frac{\partial \overline{u}}{\partial x}+v\frac{\partial \overline{u}}{\partial y}+w\frac{\partial \overline{u}}{\partial z}=\frac{1}{\rho}\frac{\partial \overline{p}}{\partial z}+2\Omega\omega\cos\theta+\Omega^2\bar{z}\cos\theta+\frac{\partial}{\partial x}\left(u\frac{\partial u}{\partial x}-\overline{w'u'}\right) \qquad (25c)$$

where (u, v, w) are the velocity components in directions (x, y, z), i.e. the axes of the local system of coordinates, and with ɵ defining the angle between the tangent to the airfoil and the x–z plane. The desired output variables are computed in some proper surfaces of constant radius, extended to a distance of half chord length from the blade wall. The variables of interest are sorted in a new order, according to the boundary layer in the tangential and normal directions. The derivatives are estimated taking a second order polynomial fitting of the output data for non–uniform spaced grids (Versteeg & Malalasakera, 1995).The boundary layer height is also found, checking both the vorticity magnitude and the velocity gradient values along the normal direction as diagnostic method. Major goal of the N–S method was ability to capture nonlinear effects without resorting to lower-fidelity methods that need empirical models to validate results.

Functions approximation is a way of obtaining relatively accurate representation of a wind turbine electrical generation dynamics, in terms of current source, capacitor and resistance. It is made by using a few parameters which represent model of wind turbine. The equation, which describes the behaviour of the wind turbine, is given by the following expression (Kaminsky et al, 2012):

$$J_m\frac{d\omega_r}{dt}+f_m+\omega_r=T_m-T_e \qquad (22)$$

where $J_m=\frac{\pi r^4}{2}=\frac{\pi D^4}{32}$

and I=J and on the basic of duality principle, mechanical variables are represented by adequate electrical quantities:

(i) Inertia constant Jm, [kg.m2] with capacitance C, [ ]
(ii) Friction coefficient fm, [N.m/(rad/s)] with conductance 1/R, [1/Ω]
(iii) Mechanical torque Tm, [N.m] with current i, Amp
(iv) Angular velocity ωr , [rad/s] with voltage, V,

Therefore, the instantaneous value of voltage (V) is equivalent to the rotor angular velocity ωr [rad/s]. The current at the machine input represents the torque shaft, which is balanced with the electromagnetic torque.

Results

The chord length and pitch angle distribution were the variables altered with the optimization of the geometric features of the wind turbine rotor to obtain optimal rotor performance. From the base study the following data was presented:

Table 1: Blade section profiles at four stations (NACA 2012).

Blade point	Wind speed range	rotor radius [m]	Pitch angle [°]	Chord [m]	Thickness [m]	Location along rotor radius [%]
1	5	0.6	9.3	0.81	0.10	20
2	6	2.2	2.7	0.55	0.06	35
3	7	3.4	0.5	0.42	0.05	65
4	8	4.2	0.2	0.38	0.03	90

Rotor radius 3.7 m, Hub radius 0.37 m, Rotational speed 80 rpm, Wind speed range (Weibull weighting distribution) 5 to 10 m/s, Wind speed with highest weighting 8 m/s

Table 2: 2D lift, drag and moment measurements

Numerical (CFD) using Fluent	Analytical (using actuator disc method)	Analytical (bending element momentum method)	Error
C_L=0.9559; C_D= 0.00137	C_L = 0.9575; C_D = 0.00135		0.0016; 0.00002
76.22 N		$F_L=0.5\rho v_r^2 C_L=0.5x1.225x11.41^2x0.9575=76.35N$	0.13
0.1092 N		$F_D=0.5\rho v_r^2 C_D=0.5x1.225x11.41^2x0.00135=0.1076N$	-0.0018
76.22 N		$F_R=(F_D^2 + F_L^2)^{1/2} = 76.35N$	0.13
P_N=620.43W		$P_A=T\omega=F_R\omega r=F_R v=76.35 \times 8.14=621.489W$ $=0.5\rho A v_o^3 C_P=0.5x1.225x7.296 \times 8^3 \times C_P$	1.459
116.159Nm		Tr=76.35x1.524=116.357Nm	0.198
0.271	C_P=621.489/2288.026 = 0.272		0.002

$\alpha = 70$; $v0 = 8$ m/s ; $N = 51$ rpm ; $r = 1.524$ m ; $\rho = 1.225$ Kg/m3, $v = r\omega = 2\pi Nr / 60 = 1.524 \times 2 \times \pi \times 51 / 60$ V = 8.14 m/s, $vr = (v2 + v02)1/2 = (8.142 + 82)1/2 = 11.41$ m/s

Two steps of CFD analysis are involved: preprocessing or meshing, done in Gambit and post processing or flow analysis, done in Fluent. Inlet wind velocity and angle of attack values are inputted into Fluent, then the values of CL and CD are evaluated. Each step of the analysis included importing the computer aided design (CAD) file into the Gambit, selecting physical models, generating a numerical mesh as in Figure 6, and applying boundary conditions. The analysis used a computational finite volume method to analyze the cases with a Fluent flow solver. The objective of the analysis was to optimize the attack angle in order to obtain the greatest possible lift force. Using gambit, approximately 500,000 cells were generated for the 2D analysis for the blade, around 750,000 cells were generated for the 2D turbine assembly, 900, 000 for the 3D blade analysis and for the full complete HAWT analysis about 1.2 million cells were used in the simulations. Figures 2, (i) to (iii) and (v) depict 2D while (iv) and (vi) 2D 3D depict grid configurations.

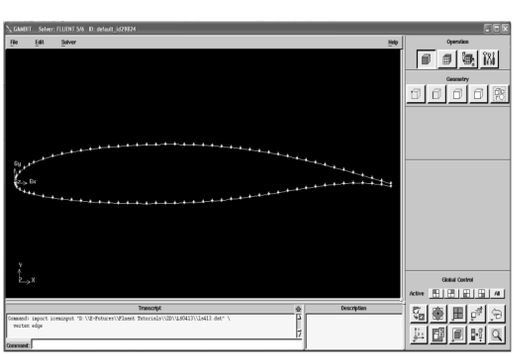

(i) 2D CAD File of the Blade in Gambit

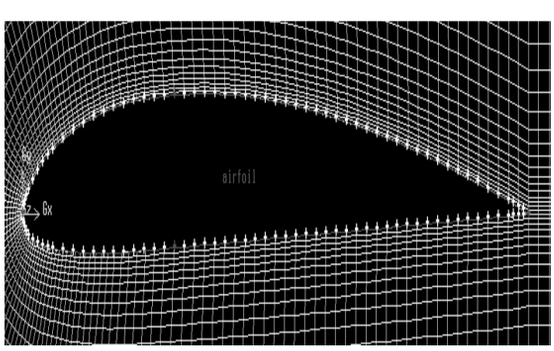

(ii): Creating Meshes on the Blade with Gambit

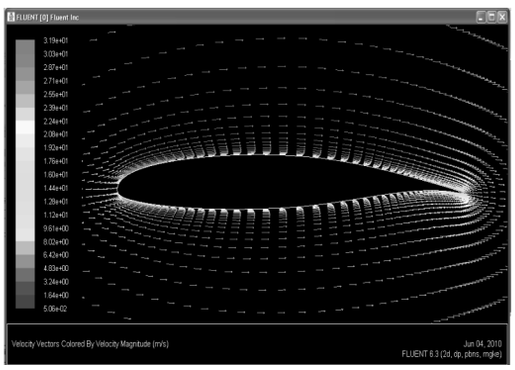

(iii): Refining the Meshes of the CFD Analysis.

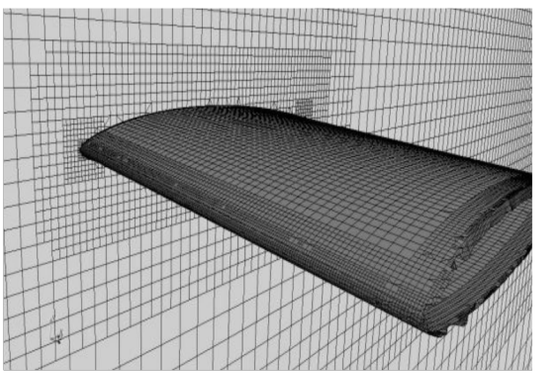

(iv) 3D Meshes on the Blade

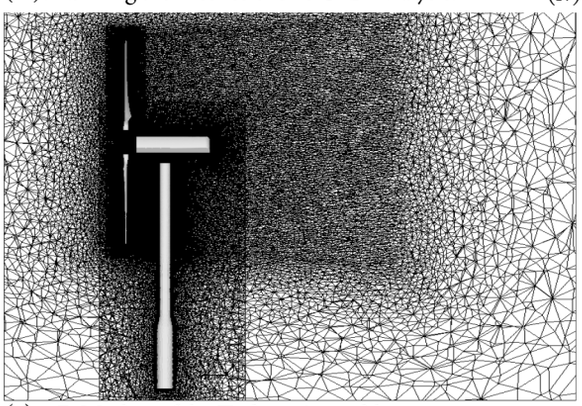

(v): 2D Meshes of the Turbine Assembly

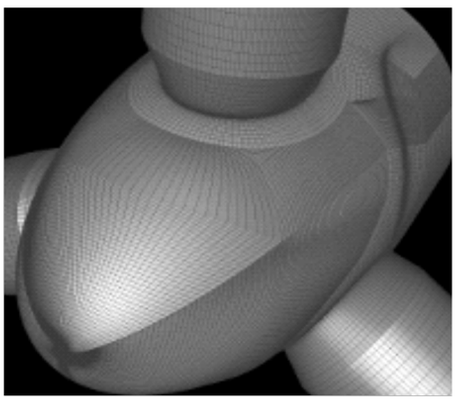

(vi) 3D Meshes of the Turbine Assembly

Figure 3: CFD modelling wind turbine blade and system

The airfoils and the full assembly were then analyzed at various angles of attack and for different wind speeds using Fluent as illustrated in Figures 7 to 8 and presenting the results as in figures 9 to 15. The full assembly included 3 airfoils that were attached into a 5m high, 2m diameter structure. Modeling of the turbulence in each of the cases was done using the 2 equation shear stress transport kinetic –omega (SST k-ω) model. This selection for the turbulence model was made because the k-ω model offers great analysis in both fully developed flow and along the boundary layer regions. Wind turbine aerodynamics involves several aspects that are unique for turbomachines: the flow past a wind turbine blade is three-dimensional, particularly in the blade-tip and root region. For instance centrifugal and Coriolis forces are experienced by the boundary layer flow, mainly in the inboard, causing a stall-delay effects, by which higher lift is achieved compared to two-dimensional data.

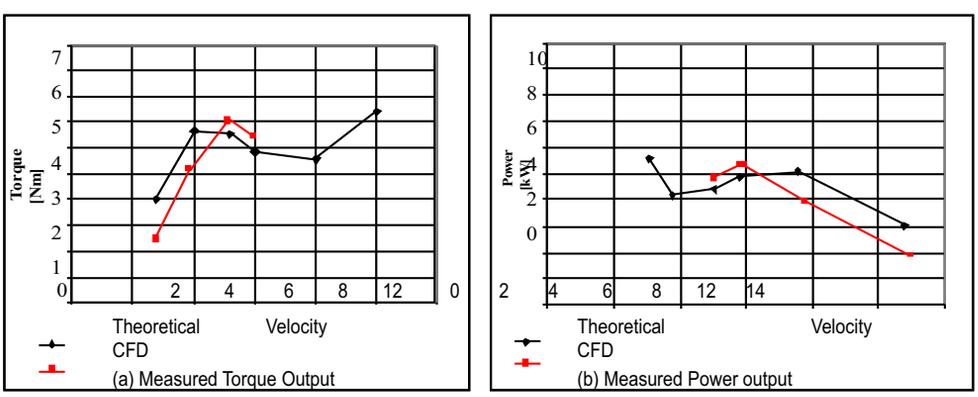

Figure 4: Results comparison between CFD and experiment

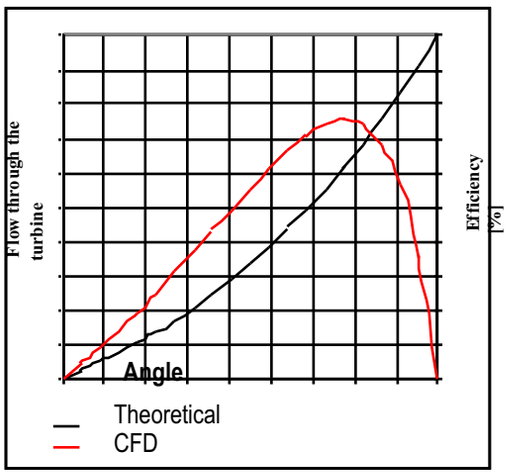

Figure 5: Efficiency and Flow through versus the pitch angle

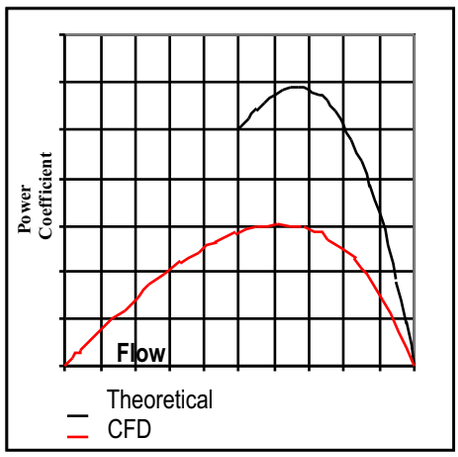

Figure 6: Power Coefficient versus Flow through the turbine

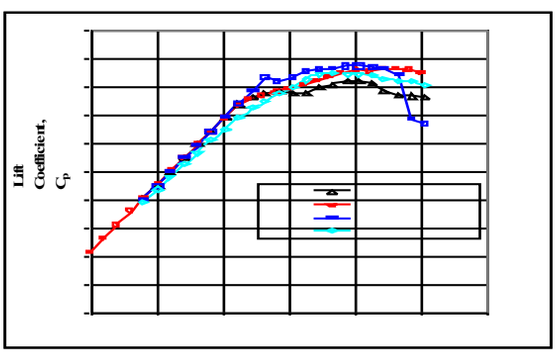

Experimental

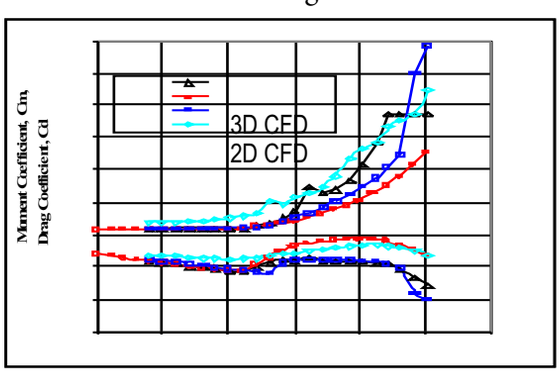

Theoretical

3D CFD
2D CFD
Experimental
Theoretical

Velocity
a. Lift Coefficient

Velocity
b, Moment and Drag Coefficients

Figure 7: Lift, Drag and Moment

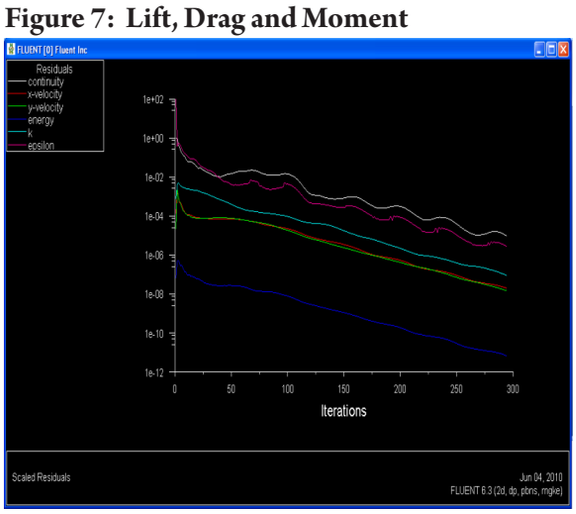

(a)

(b)

Figure 8: Results and Simulation from the Fluent Analysis.

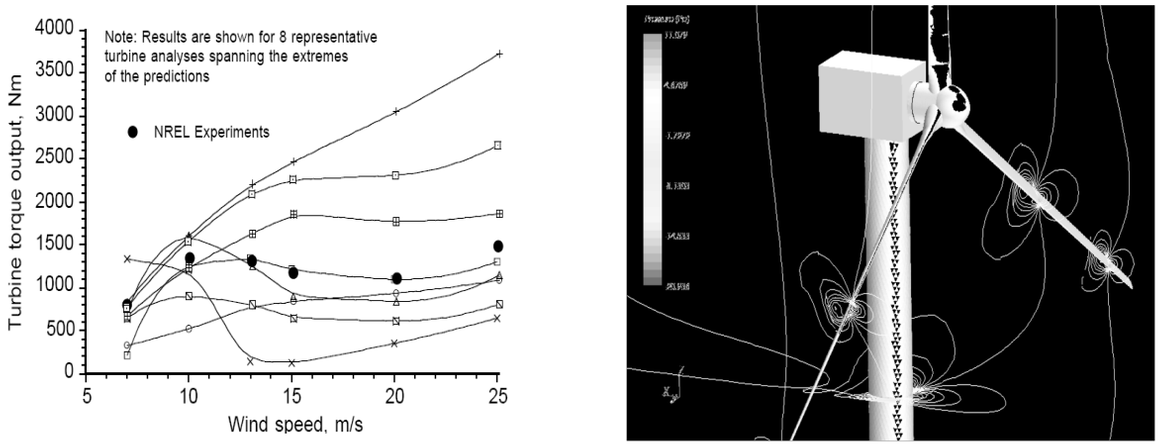

(a) (b)

Figure 9: Representative "in the blind" predictions of turbine power output as a function of wind speed compared to experimental measurements (Leishman, 2002)

Discussion

The performance of a wind turbine can be characterized by three main indicators power, torque and thrust and letting them vary with wind speed, V (see tables 1 and 2). The power determines the amount of energy captured by the rotor. The torque determines the size of the gear box. Finally, the rotor thrust has great influence on the structural design of the tower. Regarding aerodynamics and the subject of this work, the most important among the three is indeed, power. It is convenient to express the performance by means of non-dimensional, characteristic performance (power, torque and thrust coefficients) as functions of tip speed ratio and the results in table 2 indicated the accuracy involved using CFD compared to AD and BEM.

The wind turbine efficiency (Figure 5) is a key parameter in the economic viability, recovery of initial capital investment and long term profitability. Detailed calculations using the AD and BEM methods are made to show the influence of various factors such as the tip–speed ratio and blade number on performance. Further development of the theory includes the application of Prandtl's tip loss correction factor that corrects for a finite number of blades. This Glauert's optimization analysis was developed and used to determine the ideal blade shape for a given lift coefficient and to show how optimum rotor power coefficient is influenced by the choice of tip–speed ratio (Figure 7a). The value is much less than the Betz limit, due mainly to the drag and tip losses for the attached flow conditions (the simple BEM-method adopted here is indeed not able to catch them correctly, and over predicts the CP), whereas at the lower tip speed ratios is the stall, which plays a major role in reducing the overall aerodynamic efficiency. The data are not expected to match exactly, at least because the BEM-designed blade does not follow exactly the real shape of the turbine.

The first part of the analysis involved studying the effects that varying attack angles and wind speeds had on the flow regions (Figures 5 and 6). As expected, increasing the attack angle of the airfoil created larger regions of separation causing what is known as the stall effect. Increasing the wind speed caused the separation regions to be more exaggerated with a greater amount of turbulence present. This method was then shown to predict root and tip vortex locations and strengths similar to an overset method, but without the computational expense of modeling the blade surfaces. The CFD model was able to accurately predict rotor loads when stalled as can be seen in figure 8 and 9. In yawed flow, excellent correlations of mean blade

loads with experimental data were obtained across the span, and wake asymmetry and unsteadiness were also well-predicted. The Fluent was used in all the calculation presented. The same analysis that was done above on the 2D airfoil was done on the 3D airfoil model and it produced similar results as with experimental and theoretical results (see Figure 7). Figure 8 shows the velocity distribution around the airfoil. The streamlines become more turbulent as the angle of attack is increased. To validate the numerical model, the overall performances for the new designed turbine were computed and compared to BEM calculations. The shaft mechanical power as a function of the wind velocity is showed in table 2, together with the corresponding power coefficient CP as a function of the global tip speed ratio. The CFD results are found to be in good agreement with those obtained using the BEM method, for the tested undisturbed wind velocities, ranging from 5 to 10 m/s, i.e. for generally attached flow conditions. At higher wind speeds, however, there are significant discrepancies and unsteady computations are preferable.

However, it is interesting to note that the CFD computations performed with Fluent have a similar trend to the measured power curve. It is noticeable that the maximum computed value of CP is only about 0.271 (and around 0.272 regarding the measurements), achieved at the nominal wind speed of 8m/s (table 2). The thrust coefficient computed with Fluent is compared to the results from the AD method; a discrepancy was observed showing that without the assumption made with the AD method, the thrust calculated will be less. The validation of CFD against 2D/3D blade sections (Figures 8 and 9) showed that using a high resolution structured mesh, with advanced turbulence and transition models provides an excellent match with experimental data in the attached flow regime. Validation of a normal fidelity model of the 2D blade section showed a poor match in the attached flow regime, but better performance than the high fidelity 3D model beyond the peak lift point. A comparison study using AD and BEM theories have been conducted to ensure that the value of Torque from CFD and AD/BEM in this study is synchronized. This is to prove that the analysis conducted correlated to the theory of wind turbine is correct and un-doubtful.

Conclusion

The modeling of the turbine blade and assembly in both the 2D and 3D cases allows conceptualization study of the aerodynamics of various wind turbine geometries at different speeds to get a true feel for how the specific blade and turbine assembly might behave in real world applications. Wind speeds of 5-10 m/s were studied, as well as varying attack angles from 0 to 15 degrees, the results of this research on the NACA 001234 airfoil showed it could be a very viable choice for a residential wind generator.

Furthermore, utilising the same high fidelity model for a 3D case generates an extremely computationally demanding and expensive simulation. Therefore, the normal fidelity 2D model offered overall comparable performance with the high fidelity 3D model, but at a significant saving in computational power and expense. Overall, the CFD is outstanding in terms of the detail data, flow simulation, flow visualization and giving a real world flow conceptualization in virtual laboratory.

References

Gould, E.B. (2012). "Fundamentals of wind energy. National renewable energy technology." Alaska wind applications training symposium, Bethel, Alaska.

Ingram, G. (2011, October 18). "Wind turbine blade analysis using the blade element momentum method." Version 1.1. Creative Commons Attribution-Share Alike. http://creativecommons.org/licenses/by-sa/3.0/

Johnson, G. L. (2006, October 10)." Wind energy systems". Manhattan, KS.

Kaminsky, C; Filush, A; Kasprzak, P & Mokhtar, W. (2012). "A CFD study of wind turbine aerodynamics." Proceedings of the 2012 ASEE North Central Section Conference. American Society for Engineering Education.

Kishinami, K. et al (2005). "Theoretical and experimental study on the aerodynamic characteristics of a horizontal axis wind turbine" Elsevier.

Leary, J. (June, 2010). ""Mini-project report computational fluid dynamics analysis of a low cost wind turbine." The University of Sheffield.

Leishman, J. G (2002). "Challenges in Modeling the Unsteady Aerodynamics of Wind Turbines" AIAA-2002-0037.

Madsen, H.A; Mikkelsen, R; Oye, S; Bak, C. & Johansen, J. (2007). "A detailed investigation of the blade element momentum (BEM) model based on analytical and numerical results and proposal for modification of the BEM model" The Science of Making Torque from Wind, Journal of Physics: Conference Series 75.

Mahawadiwar, H. V. et al. (2012, May-June). "Cfd analysis of wind turbine blade". International Journal of Engineering Research and Applications Vol. 2 (3). 3188-3194.

Mikkelsen, R. (2003). "Actuator disk methods applied to wind turbines." A Dissertation submitted to Technical Uni. of Denmark, Fluid Mechanics, Dept. of Mech. Eng for the award of PhD.

Mughal, M. O. & Ullah, I. (2011, January 10 - 13). "Upwind horizontal axis wind turbine performance prediction by CFD analysis." Proceedings of International Bhurban Conference on Applied Sciences & Technology. Islamabad, Pakistan.

Nayir, A; Rosolowski, E. & Jedut, L. (2010, September)." New trends in wind energy modelling and wind turbine" International Journal on Technical and Physical Problems of Engineering. Issue 4 Volume 2 (3) 51-59.

Pierce, W. T. (2008). "Evaluation and Performance Prediction of a Wind Turbine Blade." M.Sc. Thesis, Department of Mechanical Engineering, University of Stellenbosch, South Africa

Piggott, H. (2012). "How to build a wind turbine." http//. Accessed on September 28, 2012.

Versteeg H.K. & Malalasakera W. (1995). "An introduction to computational fluid dynamics: the finite-volume method." Harlow, Longman Scientific & Technical, New York.

World Commission on Environment and Development, WCED (1987). "Our common future." Oxford University Press, Oxford.

World Energy Council, WEC (1993). "Energy for tomorrow"s world." St Martin"s Press: New York.

Nomenclatures, a' axial and angular induction factors

Ao	local area
AOM	annual operation and maintenance cost
Ar	rotor area
b	number of blade
c	chord length of the local blade section
C	capacitance
CD	coefficient of drag
CL	coefficient of lift
Cp	power co-efficient or capacity factor (efficiency factor)
D	diameter
F	impact force

FD drag Force
FL lift force
fm friction coefficient
GS size of the wind turbine
h,Hm height above sea level
i current
Jm Inertia constant
k shape parameter
L lift force
n number of observation in the averaging period
N speed of wind turbine
P power
PA analytical power
Pd power density
Pextracted power extracted
PN numerical power
r blade radius
t time
T thrust force
Tc thrust coefficient
Tm mechanical torque
$U\infty$ air free stream velocity
Ua axial or streamwise velocity
Ut tangential velocity
v wind inlet velocity
V voltage
v3 downstream velocity
vo outlet wind velocity
vo,vz,v_{θ} local velocity components
vr resultant wind velocity
vrel blade relative velocity
WM world map power
. wind shear
1/R conductance
r air density
α angle of attack
λ speed ratio
ρ air density
σ turbine solidity
ω, Ω blade angular velocity
Fz axial force
F0 tangential force